 CMES, vol.6, no.6, pp.525-535, 2004

Numerical Treatment of Domain Integrals without Internal Cells in Three-Dimensional BIEM Formulations

Yoshihiro Ochiai [1] **and Vladimir Sladek**[2]

Abstract: The conventional boundary element method (BEM) uses internal cells for the domain integralsCwhen solving nonlinear problems or problems with domain effects. This paper is concerned with conversion of the domain integral into boundary ones and some non-integral terms in a three-dimensional BIEM, which does not require the use of internal cells. This method uses arbitrary internal points instead of internal cells. The method is based on a three-dimensional interpolation method in this paper by using a polyharmonic function with volume distribution. In view of this interpolation method, the three-dimensional numerical integration is replaced by boundary ones and preceding calculation of some boundary densities and interior unknowns. The domain discretizetion procedure is completely eliminated. In order to investigate the efficiency of this method, several numerical examples are given.

keyword: Boundary Element Method, Domain integrals, Heat Conduction, Interpolation, Polyharmonic functions, Multiple-Reciprocity Method

1 Introduction

Recently, a great attention has been devoted to the development of various discretization methods based on meshless approximations [Atluri et al (2002, 2003), Han and Atluri (2003), Liu (2003), Atluri (2004)]. Only some of them are truly meshless. Anyway, a serious interest and valuable progress can be observed in the development of computational methods which can be named as mesh reduction method (MRM). The first recognized achievement in the development of MRM was the development of the boundary integral equation methos (BIEM) or boundary element method (BEM) [Brebbia et al (1984)]. The pure boundary integral formulation, however, is not available in general. Owing to the absence of the fundamental solutions in general nonlinear problems and/ or problems in non-homogeneous media, the fundamental solutions of simplified operators can be used with resulting into the so-called boundary-domain formulations. Then, the discretization of the domain into cells is required because of unknown field variables involved in domain integral integrands. In order to avoid the use of internal cells, multiple-reciprocity BEM and dual reciprocity BEM have been proposed [Nowak, et al.(1994). Partrige, et. al. (1991)]. The first author has already proposed an improved multiple-reciprocity BEM or triple-reciprocity BEM [Ochiai et al., (1995, 1996, 2001)]. In this method, a distributed value is interpolated using boundary integral equations and polyharmonic functions [Ochiai et al., (2001)]. On the other hand, the radial basis function (radius spline) has been proposed for use in interpolating an arbitrary distribution, and is useful for scattered data [Dyn (1987), Welch, et al. (1992)].

In this paper, a numerical multiple integration method is proposed using the proposed multidimensional interpolation method, which is based on boundary integral equations and polyharmonic functions and new polyharmonic functions with volume distribution. If a given region can be transformed into several standard regions (internal cells) for which a rule of approximate integration is available, then the integration in the given region can be computed numerically [Davis and Rabinowitz, (1984)]. In this study, the multiple integration is numerically carried out by using boundary integral equations, and the three-dimensional domain integration is transformed into a two-dimensional boundary integration. Thus one dimension is reduced by this method. This method uses arbitrary internal points instead of internal cells, and requires values on a boundary of a region and values at arbitrary internal points. This method is based on a modified multiple-reciprocity BEM (triple-reciprocity BEM) for heat conduction analysis with heat generation [Ochiai et al., (1995, 1996)]. This integration is effective for

[1] Dept. of Mech. Eng., Kinki University, Kowakae 3-4-1, Higashi-Osaka, 577-8502 Japan, E-Mail: ochiai@mech.kindai.ac.jp
[2] Institute of Construction and Architecture, Slovak Academy of Science, 845 03 Bratislava, Slovakia

boundary-domain formulations because internal cells are not required for computation of domain integrals. Thus, it is useful for solving inelastic problems and for thermal stress analysis with arbitrary internal heat generation. Several examples are given in order to investigate the efficiency of this method.

2 Theory

2.1 Domain integral

In BEM formulations, we have often to deal with the domain integral [Brebbia, et al.(1986)]

$$I(p) = \int_{\Omega} F_1(p,q) W_1(q) d\Omega \tag{1}$$

where Ω is a domain. The functions $F_1(p,q)$ and $W_1(q)$ are an integral kernel and an arbitrary distributed function, respectively. The notations p and q are respectively an observation point and a loading point. The distribution of function $W_1(q)$ throughout the domain is assumed to be known a priori.

2.2 Interpolation using polyharmonic function

In order avoid the use of domain integral, an interpolation method using boundary integrals is introduced. The following equations can be used in the three-dimensional interpolation [Ochiai et al. (1996, 2000, 2001)]:

$$\nabla^2 W_1 = -W_2 \tag{2}$$

$$\nabla^2 W_2(q) \approx -\sum_{m=1}^{M} W_{3m} \chi_m(q), \quad q,\ q_m \in \Omega \tag{3}$$

The support function $\chi_m(q)$ is defined as

$$chi_{m(q)}(q) = \begin{cases} 1, & if \quad |q-q_m| \le A \\ 0, & if \quad |q-q_m| > A \end{cases} \tag{4}$$

where A being the radius of spherical support domain. The interior nodal values W_{3m} are unknown. From Eqs.(2) and (3), the following equation can be obtained.

$$\nabla^4 W_1 = \sum_{m=1}^{M} W_{3m} \chi_m(q) \tag{5}$$

We shall assume W_2=0 on the boundary. Equations (2) and (3) are solved using boundary integral equations. Then, a polyharmonic function T_f is introduced.

$$T_f(P,Q) = \frac{r^{2f-3}}{4\pi(2f-2)!}, \quad (f = 1,2,3,.....),$$
$$r = |P-Q| \tag{6}$$

The polyharmonic functions obey the following relation

$$\nabla^2 T_{f+1} = T_f \quad \text{with} \quad \nabla^2 T_1(r) = -\delta(r) \tag{7}$$

The polyharmonic function with volume distribution T_{fA}, which expresses the state of the uniformly distributed polyharmonic function T_f in a spherical region with radius A, as shown in Fig.1, is introduced in order to obtain a smooth interpolation [Ochiai (2001)].

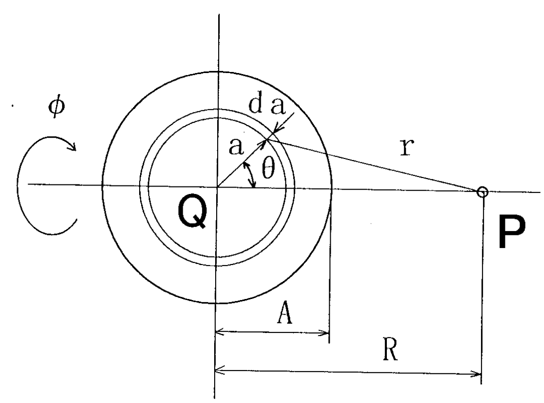

Figure 1 : Notations for polyharmonic function with volume distribution

$$T_{fA}(P,Q) = \int_0^A \int_0^{2\pi} \int_0^{\pi} T_f(P,q) a^2 \sin\theta d\theta d\phi da \tag{8}$$

The polyharmonic functions with volume distribution T_{fA} , as shown in Fig. 2, can be explicitly shown as

$$T_{1A} = \frac{A^3}{3r} \qquad r > A, \tag{9}$$

$$T_{1A} = \frac{3A^2 - r^2}{6} \qquad r \le A, \tag{10}$$

$$T_{2A} = \frac{A^3}{6r}(r^2 + \frac{A^2}{5}) \qquad r > A, \tag{11}$$

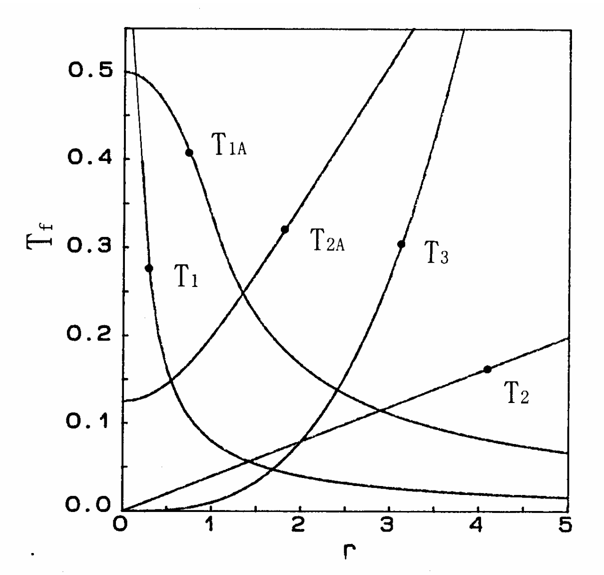

Figure 2 : Polyharmonic function T_f and Polyharmonic function with volume distribution T_{fA}

$$T_{2A} = -\frac{r^4 - 15A^4 - 10r^2A^2}{120} \qquad r \leq A. \tag{12}$$

The polyharmonic functions with volume distribution T_{fA} obey the next relation

$$\nabla^2 T_{f+1A} = T_{fA}. \tag{13}$$

On the other hand, the density of W_1 can be expressed using the Gauss divergence theorem two times and Eqs.(2), (3), (7) and (13) as follows:

$$cW_1(p) = -\sum_{f=1}^{2}(-1)^f \int_{\partial\Omega}\{T_f(p,Q)\frac{\partial W_f(Q)}{\partial n} - \frac{\partial T_f(p,Q)}{\partial n}W_f(Q)\}d\Gamma(Q) - \sum_{m=1}^{M} T_{2A}(p,q_m)W_{3m} \tag{14}$$

where $\partial\Omega$ is the boundary of the domain, $c = 0.5$ on the smooth boundary and $c = 1$ in the domain. Furthermore, W_2 starting Eq.(3), the boundary density $W_2(P)$ can be expressed as

$$cW_2(P) = \int_{\partial\Omega}\{T_1(P,Q)\frac{\partial W_2(Q)}{\partial n} - \frac{\partial T_1(P,Q)}{\partial n}W_2(Q)\}d\Gamma(Q) + \sum_{m=1}^{M} T_{1A}(P,q_m)W_{3m} \tag{15}$$

Approaching the interior point p and q to the boundary, we shall use the capital letter P and Q, respectively.

According to Eq.(14) the function $W_1(p)$ is represented in terms of W_{3m} and boundary densities $W_f(Q)$ and $\partial W_f(Q)/\partial n$. Since $W_1(Q)$ is known and $W_2(Q) = 0$, we need to compute $\partial W_f(Q)/\partial n$ and W_{3m} before using the representation by Eq.(14). For this purpose we can used Eqs.(14) and (15) collocated at boundary points P as well as Eq.(14) collocated at interior nodes q_m. Constant elements are used for the boundary. Replacing W_f and $\partial W_f/\partial n$ by vectors W_f and V_f, respectively, and discretizing Eq.(14), we obtain [Ochiai et al (1995, 1996)]

$$\mathbf{H}_1\mathbf{W}_1 = \mathbf{G}_1\mathbf{V}_1 + \mathbf{H}_2\mathbf{W}_2 - \mathbf{G}_2\mathbf{V}_2 - \mathbf{G}_2^{\mathrm{I}}\mathbf{W}_3^{P}, \tag{16}$$

where $\boldsymbol{H_1}$, $\boldsymbol{G_1}$, $\boldsymbol{H_2}$, $\boldsymbol{G_2}$ and $\boldsymbol{G_2^I}$ are the matrices with the following elements for a given boundary point 'i' [Brebbia, et al.(1986)]:

$$H_{1ij} = \frac{1}{2}\delta_{ij} + \int_{\Gamma_j}\frac{\partial T_1(P_i,Q)}{\partial n}d\Gamma_j(Q), \tag{17}$$

$$G_{1ij} = \int_{\Gamma_j} T_1(P_i,Q)d\Gamma_j(Q), \tag{18}$$

$$H_{2ij} = \int_{\Gamma_j}\frac{\partial T_2(P_i,Q)}{\partial n}d\Gamma_j(Q), \tag{19}$$

$$G_{2ij} = \int_{\Gamma_j} T_2(P_i,Q)d\Gamma_j(Q), \tag{20}$$

$$G^I_{2ij} = T_{2A}(P_i,q_j), \tag{21}$$

where the upper index I in Eq. (21) is related to contribution from interior nodes. The discretized form of Eq.(15) is given as follows:

$$\mathbf{H}_1\mathbf{W}_2 = \mathbf{G}_1\mathbf{V}_2 + \mathbf{G}_1^{\mathrm{I}}\mathbf{W}_3, \tag{22}$$

where $\boldsymbol{G_1^I}$ is a matrix with the following elements:

$$G^I_{1ij} = T_{1A}(P_i,q_j) \tag{23}$$

In the same manner, using the vector notation $\mathbf{W}_1^I$ for function values $W_1(p_i)$ at internal points, from Eq.(14) we obtain

$$\mathbf{W}_1^I = -\mathbf{H}_3\mathbf{W}_1 + \mathbf{G}_3\mathbf{V}_1 + \mathbf{H}_4\mathbf{W}_2 - \mathbf{G}_4\mathbf{V}_2 - \mathbf{G}_3^{\mathbf{I}}\mathbf{W}_3 \,, \tag{24}$$

where $\boldsymbol{H_3}$, $\boldsymbol{G_3}$, $\boldsymbol{H_4}$, $\boldsymbol{G_4}$ and $\boldsymbol{G_3^I}$ are the matrices with the following elements

$$H_{3ij} = \int_{\Gamma_j} \frac{\partial T_1(p_i,Q)}{\partial n} d\Gamma_j(Q) \,, \tag{25}$$

$$G_{3ij} = \int_{\Gamma_j} T_1(p_i,Q) d\Gamma_j(Q) \,, \tag{26}$$

$$H_{4ij} = \int_{\Gamma_j} \frac{\partial T_2(p_i,Q)}{\partial n} d\Gamma_j(Q) \,, \tag{27}$$

$$G_{4ij} = \int_{\Gamma_j} T_2(p_i,Q) d\Gamma_j(Q) \,, \tag{28}$$

$$G_{3ij}^I = T_{2A}(p_i,q_j) \,. \tag{29}$$

In according with the assumption $\boldsymbol{W_2} = \mathbf{0}$, Eqs.(16), (22) and (24) yield the following system of equations for unknowns $\boldsymbol{V_1}, \boldsymbol{V_2}$ and $\boldsymbol{W_3}$.

$$\begin{bmatrix} \mathbf{G}_1 & -\mathbf{G}_2 & -\mathbf{G}_2^{\mathbf{I}} \\ \mathbf{0} & \mathbf{G}_1 & \mathbf{G}_1^{\mathbf{I}} \\ \mathbf{G}_3 & -\mathbf{G}_4 & -\mathbf{G}_3^{\mathbf{I}} \end{bmatrix} \begin{Bmatrix} \mathbf{V}_1 \\ \mathbf{V}_2 \\ \mathbf{W}_3 \end{Bmatrix} = \begin{Bmatrix} \mathbf{H}_1\mathbf{W}_1 \\ \mathbf{0} \\ \mathbf{H}_3\mathbf{W}_1 + \mathbf{W}_1^{\mathbf{I}} \end{Bmatrix} \tag{30}$$

In the same manner, $\boldsymbol{V_2} = \mathbf{0}$ can be assumed on a symmetric axis in order to interpolate the symmetric distribution. When using constant elements and dividing the boundary into N_o elements and M internal points, the simultaneous linear algebraic equations with $(2N_o + M)$ unknowns must be solved.

2.3 Numerical Integration

Making use of the representation of $W_1(p)$ in term of $\boldsymbol{V_1}$, $\boldsymbol{V_2}$ and $\boldsymbol{W_3}$, one can express also an arbitrary integral (1) in terms of the same quantities. For this purpose, the new function F_{f+1} is introduced by

$$\nabla^2 F_{f+1} = F_f \,. \tag{31}$$

The function F_{fA} is introduced in according with Eq. (8) as follows:

$$F_{fA}(P,Q) = \int_0^A \int_0^{2\pi} \int_0^{\pi} F_f(P,q) a^2 \sin\theta d\theta d\phi da. \tag{32}$$

Using Eq.(31) and the Gauss divergence theorem, the following equation is obtained in view of Eqs. (2) and (3)

$$\begin{aligned} I(p) &= \int_\Omega \nabla^2 F_2(p,q) W_1(q) d\Omega = \int_{\partial\Omega} \left\{ -F_2(p,Q) \frac{\partial W_1(Q)}{\partial n} \right. \\ &\left. + \frac{\partial F_2(p,Q)}{\partial n} W_1(Q) \right\} d\Gamma(Q) + \int_\Omega F_2(p,q) \nabla^2 W_1(q) d\Omega(q) \\ &= \sum_{f=1}^{2} (-1)^f \int_{\partial\Omega} \{ F_{f+1}(p,Q) \frac{\partial W_f(Q)}{\partial n} \\ &- \frac{\partial F_{f+1}(p,Q)}{\partial n} W_f(Q) \} d\Gamma(Q) \\ &+ \sum_{m=1}^{M} F_{3A}(p,q_m) W_{3m}. \end{aligned} \tag{33}$$

Thus, the considered domain integral is replaced by boundary integrals and a sum with precomputed boundary densities and interior nodal values W_{3m}. The domain discretization procedure is completely eliminated. Using Eq.(31), the function F_{f+1} in $n-$dimensions is obtained as

$$F_{f+1} = \int \frac{1}{r^{n-1}} \left[\int r^{n-1} F_f dr \right] dr \quad , \tag{34}$$

.
provided that F_f is dependent only on $r = |P - Q|$.
First, the following function is considered.

$$F_1(p,q) = \frac{1}{r^k} (k \neq 2,3,4,5) \tag{35}$$

where k is a real number. Substituting Eq.(35) into Eq.(34), we obtain

$$F_2 = \frac{1}{(2-k)(3-k)r^{k-2}} \,, \tag{36}$$

$$F_3 = \frac{1}{(2-k)(3-k)(4-k)(5-k)r^{k-4}} \,. \tag{37}$$

Differentiating Eq.(36) with respect to normal vector n on a boundary, we obtain

$$\frac{\partial F_2}{\partial n} = \frac{r^{1-k}}{(3-k)} \frac{\partial r}{\partial n} \quad . \tag{38}$$

$$\frac{\partial F_3}{\partial n} = \frac{r^{3-k}}{(2-k)(3-k)(5-k)} \frac{\partial r}{\partial n} \tag{39}$$

Substituting Eq. (37) into Eq. (32), we obtain

$$F_{3A} = \frac{2\pi}{r}[\{(7-k)A-r\}(A+r)^{7-k} + \{(7-k)A+r\}(-A+r)^{7-k}]\prod_{\ell=2}^{8}\frac{1}{\ell-k} \quad r>A, \tag{40}$$

$$F_{3A} = \frac{2\pi}{r}[\{(7-k)A-r\}(A+r)^{7-k} - \{(7-k)A+r\}(A-r)^{7-k}]\prod_{\ell=2}^{8}\frac{1}{\ell-k} \quad r\le A. \tag{41}$$

The parameter k can be a negative real number. If the parameter $k>3$, the observation point p must be out of the domain Ω. If k=0, Eq.(1) becomes

$$I = \int_{\Omega} W_1(q)d\Omega, \tag{42}$$

because $F_1(p,q)=1$. In this case, the integral value I is not dependent on the observation point p [Ochiai (2001)]. The point p can be out of the domain. From Eqs. (36)-(40), we obtain

$$F_2 = \frac{r^2}{6}, \tag{43}$$

$$F_3 = \frac{r^4}{120}, \tag{44}$$

$$\frac{\partial F_2}{\partial n} = \frac{r}{3}\frac{\partial r}{\partial n}, \tag{45}$$

$$\frac{\partial F_3}{\partial n} = \frac{r^3}{30}\frac{\partial r}{\partial n}, \tag{46}$$

$$F_{3A} = \frac{\pi A^3}{630}(3A^4+14A^2r^2+7r^4). \tag{47}$$

In the other frequently occurring case, the integral kernel is given as follows:

$$F_1 = \frac{1}{r^k}r_{,i}\,(k\neq 1,3,4,6 \text{ real number}), \tag{48}$$

where $r_{,i}=\partial r/\partial x_i$. Differentiating Eqs. (36), (37), (39) and (40), we obtain

$$F_2 = \frac{1}{(1-k)(4-k)r^{k-2}}r_{,i}, \tag{49}$$

$$\frac{\partial F_2}{\partial n} = \frac{1}{(4-k)r^{k-1}}\left[\frac{n_i}{(1-k)}+\frac{\partial r}{\partial n}r_{,i}\right], \tag{50}$$

$$F_3 = \frac{r^{4-k}}{(1-k)(3-k)(4-k)(6-k)}r_{,i}, \tag{51}$$

$$\frac{\partial F_3}{\partial n} = \frac{r^{3-k}}{(1-k)(3-k)(4-k)(6-k)}\left[n_i+(3-k)\frac{\partial r}{\partial n}r_{,i}\right], \tag{52}$$

$$F_{3A} = \frac{2\pi(8-k)r_{,i}}{(1-k)r^2}[-A\{(A+r)^{8-k} + (-A+r)^{8-k}\} + r\{(8-k)A-r\}(A+r)^{7-k} + r\{(8-k)A+r\}(-A+r)^{7-k}]\prod_{\ell=2}^{8}\frac{1}{\ell-k+1} \quad r>A, \tag{53}$$

$$F_{3A} = \frac{2\pi(8-k)r_{,i}}{(1-k)r^2}[-A\{(A+r)^{8-k} - (A-r)^{8-k}\} + r\{(8-k)A-r\}(A+r)^{7-k} + r\{(8-k)A+r\}(A-r)^{7-k}]\prod_{\ell=2}^{8}\frac{1}{\ell-k+1} \quad r\le A. \tag{54}$$

where n_i is the component of the unit normal vector.

The next considered case is specified by the kernel

$$F_1 = \frac{1}{r^k}r_{,i}r_{,j} \quad (k\neq 0,2,3,4,5,7 \text{ real number}). \tag{55}$$

Differentiating Eq.(35) with respect to x_i and x_j, we obtain

$$\frac{\partial^2}{\partial x_i\partial x_j}F_1 = \frac{-k\delta_{ij}}{r^{k+2}}+\frac{k(k+2)}{r^{k+2}}r_{,i}r_{,j}. \tag{56}$$

Differentiating Eq.(36) with respect to x_i and x_j and adding the term for the first term in Eq.(53), we obtain

$$F_2 = \frac{1}{r^{k-2}k(5-k)}\left[\frac{2\delta_{ij}}{(2-k)(3-k)}-r_{,i}r_{,j}\right]. \tag{57}$$

In the same manner, we obtain

$$\frac{\partial F_2}{\partial n} = \frac{r^{1-k}}{k(5-k)}\left[\left\{\frac{2\delta_{ij}}{3-k}+kr_{,i}r_{,j}\right\}\frac{\partial r}{\partial n}-n_jr_{,i}-n_ir_{,j}\right], \tag{58}$$

$$F_3 = \frac{r^{4-k}}{k(2-k)(5-k)(7-k)}\left[\frac{4\delta_{ij}}{(3-k)(4-k)}-r_{,i}r_{,j}\right], \tag{59}$$

$$\frac{\partial F_3}{\partial n} = \frac{r^{3-k}}{k(2-k)(5-k)(7-k)} \left[\left\{ \frac{4\delta_{ij}}{3-k} + (k-2) r_{,i} r_{,j} \right\} \frac{\partial r}{\partial n} - n_j r_{,i} - n_i r_{,j} \right] \tag{60}$$

$$\begin{aligned} F_{3A} = & \frac{-2\pi(9-k)}{(2-k)kr^3} \langle \delta_{ij}[-A\left\{(A+r)^{9-k} + (-A+r)^{9-k}\right\} \\ & + r\{(9-k)A - r\}(A+r)^{8-k} \\ & + r\{(9-k)A + r\}(-A+r)^{8-k}] \\ & + r_{,i} r_{,j} [3A\{(A+r)^{9-k} + (-A+r)^{9-k}\} \\ & - r\{3(9-k)A - r\}(A+r)^{8-k} \\ & - r\{3(9-k)A + r\}(-A+r)^{8-k} \\ & + r^2\{(9-k)A - r\}(8-k)(A+r)^{7-k} \\ & + r^2\{(9-k)A + r\}(8-k)(-A+r)^{7-k}] \rangle \\ & \prod_{\ell=2}^{8} \frac{1}{\ell-k+2} + \frac{2\pi\delta_{ij}}{kr}[\{(7-k)A - r\}(A+r)^{7-k} \\ & + \{(7-k)A + r\}(-A+r)^{7-k}] \prod_{\ell=2}^{8} \frac{1}{\ell-k} \qquad r > A, \end{aligned} \tag{61}$$

$$\begin{aligned} F_{3A} = & \frac{-2\pi(9-k)}{(2-k)kr^3} \langle \delta_{ij}[-A\{(A+r)^{9-k} - (A-r)^{9-k}\} \\ & + r\{(9-k)A - r\}(A+r)^{8-k} \\ & + r\{(9-k)A + r\}(A-r)^{8-k}] \\ & + r_{,i} r_{,j} [3A\{(A+r)^{9-k} + (A-r)^{9-k}\} \\ & - r\{3(9-k)A - r\}(A+r)^{8-k} \\ & - r\{3(9-k)A + r\}(A-r)^{8-k} \\ & + r^2\{(9-k)A - r\}(8-k)(A+r)^{7-k} \\ & - r^2\{(9-k)A + r\}(8-k)(A-r)^{7-k}] \rangle \\ & \prod_{\ell=2}^{8} \frac{1}{\ell-k+2} + \frac{2\pi\delta_{ij}}{kr}[\{(7-k)A - r\}(A+r)^{7-k} \\ & - \{(7-k)A + r\}(A-r)^{7-k}] \prod_{\ell=2}^{8} \frac{1}{\ell-k} \qquad r \le A\,. \end{aligned} \tag{62}$$

3 Numerical example

Examples for this interpolation using values at internal points and on a boundary are shown. Figures 3(a) and (b) show the surface and inner points of a bottle and a fictitious boundary box.

The values on the bottle surface and at inner points are assumed as 0 and –1, respectively. The value on the boundary box is +1, and Fig.3(c) shows obtained contour lines. Figures 4(a) and (b) show two obtained surfaces of the bottle using polyharmonic function with volume distribution T_{2A} and polyharmonic function T_2, respectively.

These figures show that a smoother interpolation can be obtained by using polyharmonic function with volume distribution T_{2A}. For the complicated example, Fig. 5 (a) and (b) show given surface points on a statue and the shape obtained by ray casting method [Welch (1992)].

An example of numerical integration, which has an exact value, is shown. To confirm the accuracy of the present method, the integral of the distributed function in three dimensions for a spherical region with radius a=10 mm, as shown in Fig.6, is obtained. The function is given by

$$I_1 = \int_\Omega \frac{B^2 - r^2}{B^2} d\Omega \tag{63}$$

where r is the distance from the center. Figures 6(a) and (b) show the square boundary elements and the arbitrary internal points used for interpolation. The exact value obtained from Eq.(58) is I_1=8πB^3/15 =1675.516. . . , and the numerical value obtained by Eqs.(41) and (45), is 1691.04. Constant boundary elements are used for these calculations. Similarly, the next value is obtained using Eq.(52) in the case of k=1:

$$I_2 = \int_\Omega \frac{r_{,x} r_{,x}}{r} \frac{B^2 - r^2}{B^2} d\Omega \tag{64}$$

Equations (57) and (58) become

$$\begin{aligned} F_{3A} = & \frac{-\pi A^3}{5670}[\delta_{ij}(\frac{A^6}{r^3} + 189A^2 r + 210 r^3) \\ & - 3 r_{,i} r_{,j} (\frac{A^6}{r^3} - 9\frac{A^4}{r} + 63A^2 r + 105 r^3)] \quad r > A, \end{aligned} \tag{65}$$

$$\begin{aligned} F_{3A} = & \frac{\pi}{11340}[\delta_{ij}(105A^6 + 567A^4 r^2 + 135A^2 r^4 - 7r^6) \\ & - 12 r^2 r_{,i} r_{,j} (63A^4 + 18A^2 r^2 - r^4)] \qquad r \le A \end{aligned} \tag{66}$$

The exact value obtained from Eq.(60) is I_1=104.719, and the numerical value obtained by Eq.(33), assuming k=1, is 106.121.

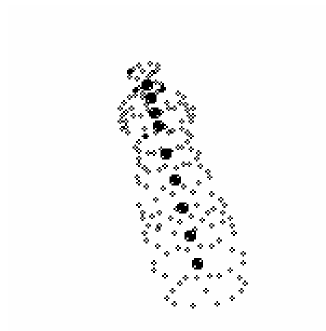

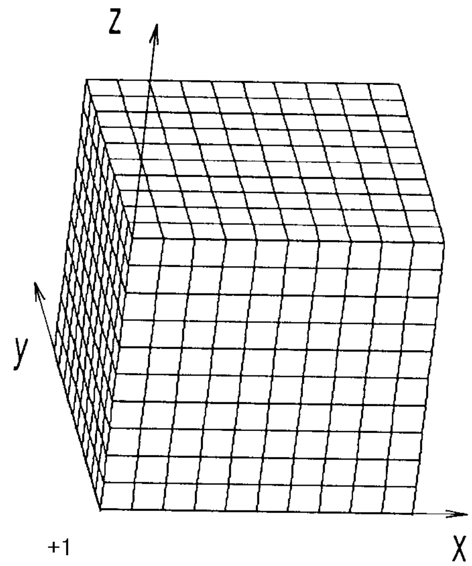

(a) Internal points (Surface: 0, Inner points: –1) (b) Boundary element (+1)

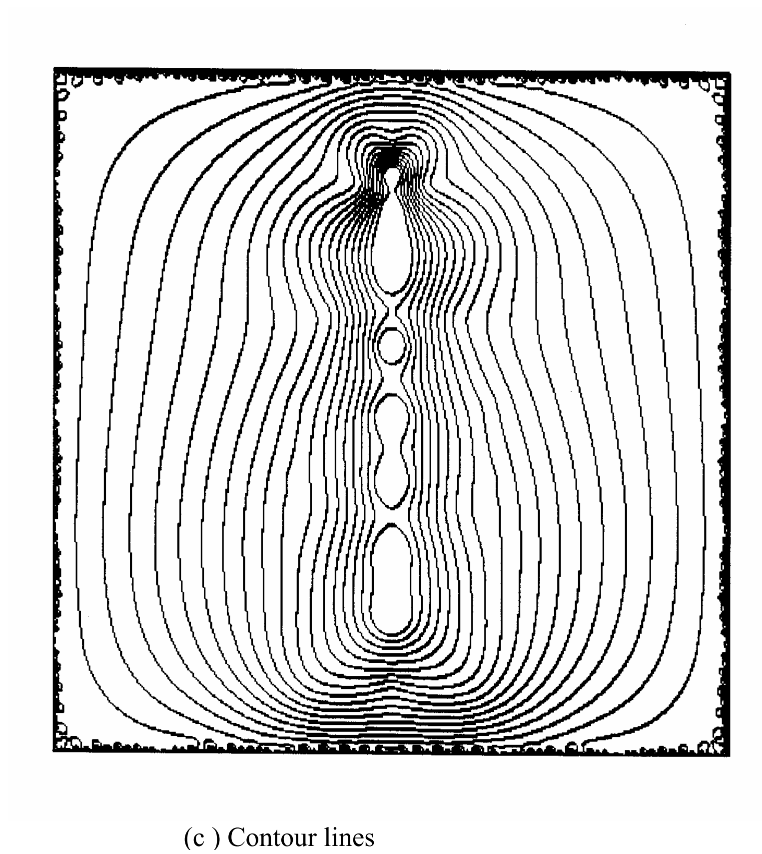

(c) Contour lines

Figure 3 : Example of interpolation using boundary integral equations

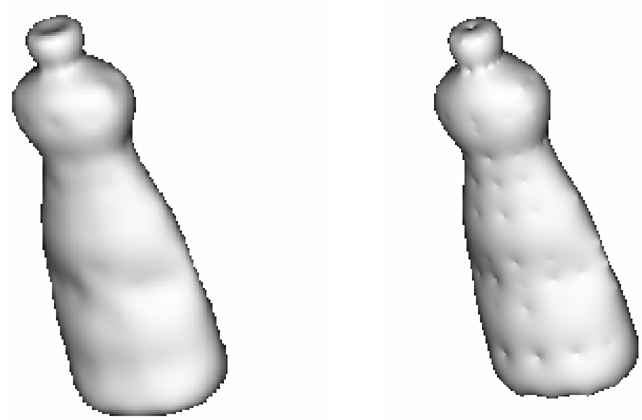

(a) T_{2A} (b) T_2

Figure 4 : Surfaces with value 0 using ray casting

The integral of a distributed function in three dimensions for a cubic region with side length L=10 mm, as shown in Fig.7(a), is obtained. The function is given by

$$I_3 = \int_\Omega r r_{,x} \sin(\frac{x\pi}{L}) \sin(\frac{y\pi}{L}) \sin(\frac{z\pi}{L}) d\Omega, \tag{67}$$

where r is the distance from origin (0, 0, 0). Figure 3 (b) shows internal points. Assuming k= -1 in Eq. (46), Eqs. (50) and (51) become the following same function:

$$F_{3A} = \frac{r_{,i} \pi A^3 r (5A^4 + 14A^2 r^2 + 5r^4)}{1050}. \tag{68}$$

The numerical value using a double exponential formura is I_1=1290.061, and the numerical value obtained is 1291.005.

Next, a steady temperature and temperature gradient distribution in a hollow cylindrical region with heat generation, as shown in Fig.8, is obtained using the BEM. The heat generation W_1 is given by

$$W_1 = W_0 \frac{b^2 - r^2}{b^2 - a^2}, \tag{69}$$

where a, b and r are inner and outer radii and the distance from the z axis, respectively. The upper and lower boundaries are thermally insulated. It is assumed that a=10 mm, b=30 mm and the inner and outer surfaces are 0°. Heat conduction is λ, and $W_0/\lambda = 0.1^\circ \cdot \mathrm{mm}^{-1}$ is also assumed. Temperature T is obtained using the boundary

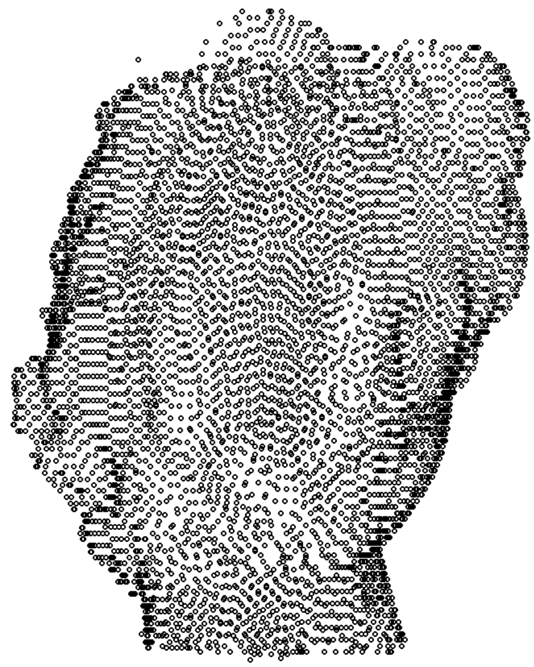

(a) Internal points

(b) Obtained shape

Figure 5 : Example of complicated interpolation

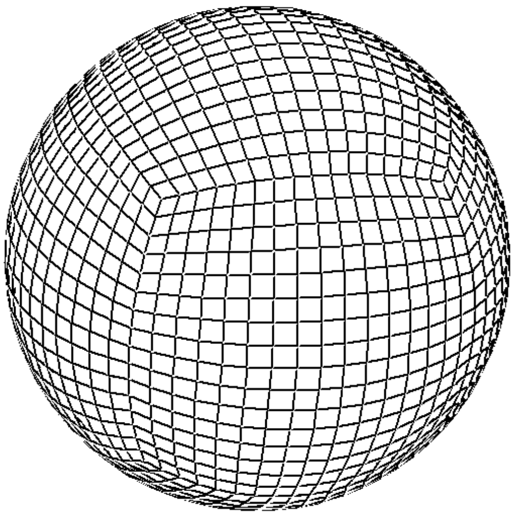

(a) Boundary elements

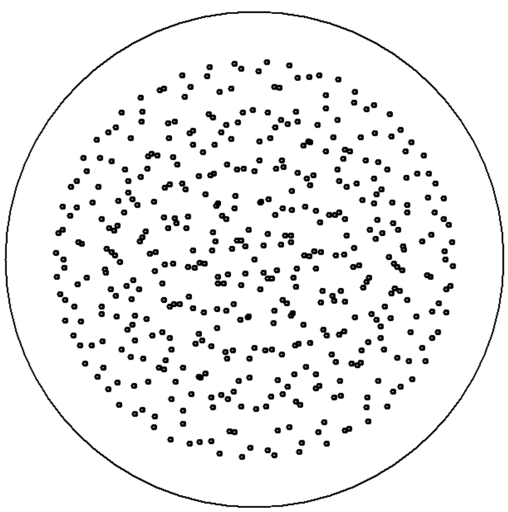

(b) Internal points

Figure 6 : Spherical region

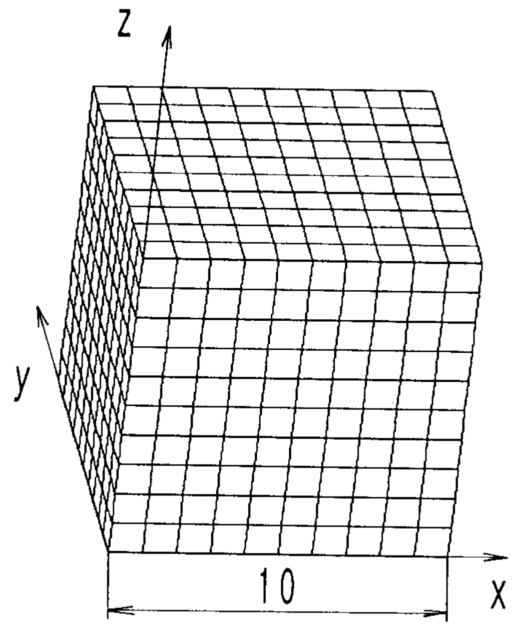

(a) Boundary elements

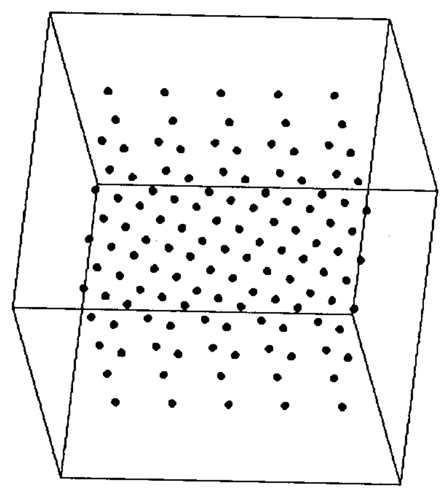

(b) Internal points

Figure 7 : Cubic region

integral equation [Brebbia, et al.(1986)]:

$$cT(P) = \int_{\partial\Omega} \{T_1(P,Q)\frac{\partial T(Q)}{\partial n} - \frac{\partial T_1(P,Q)}{\partial n}T(Q)\}d\Gamma(Q) + \frac{1}{4\pi\lambda}\int_{\Omega}(\frac{1}{r})W_1\,d\Omega \qquad (70)$$

Assuming k=1 in Eq.(35), the domain integral in Eq.(70) is calculated. Eqs. (40) and (41) become

$$F_{3A} = \frac{\pi A^3}{630r}(3A^4 + 42A^2r^2 + 35r^4) \qquad r > A\,, \qquad (71)$$

$$F_{3A} = \frac{\pi}{1260}(35A^6 + 105A^4r^2 + 21A^2r^4 - r^6) \qquad r \le A\,. \qquad (72)$$

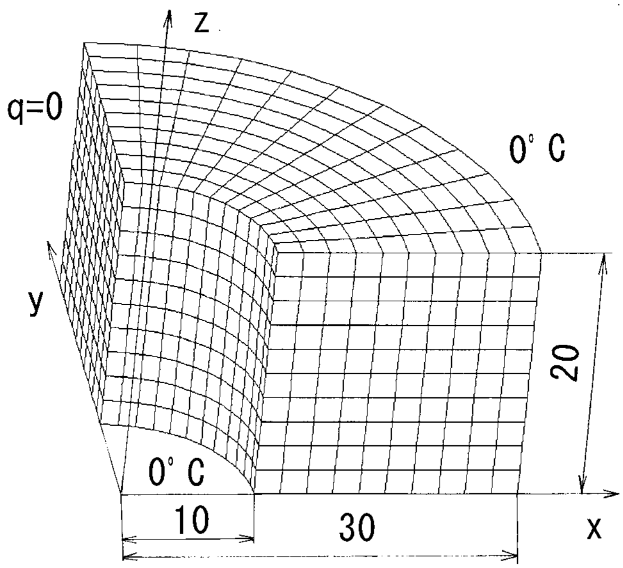

(a) Boundary elements

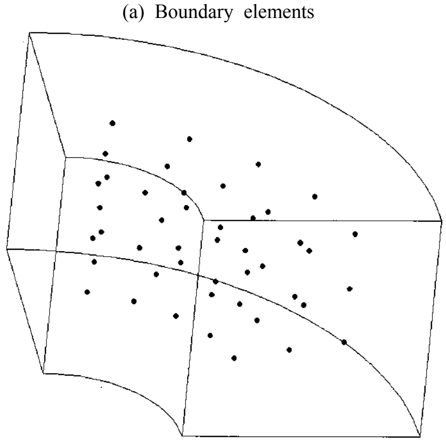

(b) Internal points

Figure 8 : Cylindrical region (quarter region)

The temperature gradient in x_i direction is obtained by

$$\frac{\partial T(p)}{\partial x_i} = \int_{\partial\Omega} \{ \frac{\partial T_1(p,Q)}{\partial x_i} \frac{\partial T(Q)}{\partial n} - \frac{\partial^2 T_1(p,Q)}{\partial n \partial x_i} T(Q) \} d\Gamma(Q) - \frac{1}{4\pi\lambda} \int_{\Omega} \frac{1}{r^2} r_{,i} W_1 \, d\Omega . \tag{73}$$

The domain integral in Eq.(73) involves the kernel given by Eq.(48) with k=2. Assuming k=2 in Eq.(43), the domain integral in Eq.(73) is calculated using Eq.(33). Eqs.

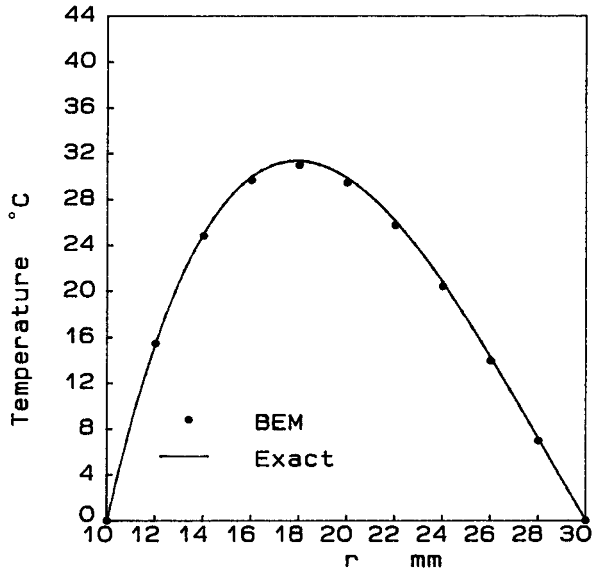

Figure 9 : Temperature distribution

(53) and (54) become

$$F_{3A} = \frac{-\pi r_{,i} A^3(-A^4 + 14A^2 r^2 + 35r^4)}{210 r^2} \qquad r > A , \tag{74}$$

$$F_{3A} = \frac{-\pi r_{,i} r(35A^4 + 14A^2 r^2 - r^4)}{210} \qquad r \leq A . \tag{75}$$

Figure 9 show the temperature distribution obtained by this method. The solid line is the exact solution. Figure 10 show the temperature gradient distribution.

Constant boundary elements are used in order to easily produce a three-dimensional program. A higher accuracy of numerical integration is achieved by using higher order boundary elements.

4 Conclusion

A numerical treatment of domain integrals in 3-D boundary integral formulations has been proposed without the need to discretize the interior of the domain. Thus, the 3-D boundary element implementation is applicable even to integral formulations involving domain integrals. It has been demonstrated that the integration using proposed approach is useful for a domain integral in an arbitrary domain, because the domain discretizetion procedure is completely eliminated. Numerical examples have shown that the presented interpolation and integral method will be useful in industrial fields.

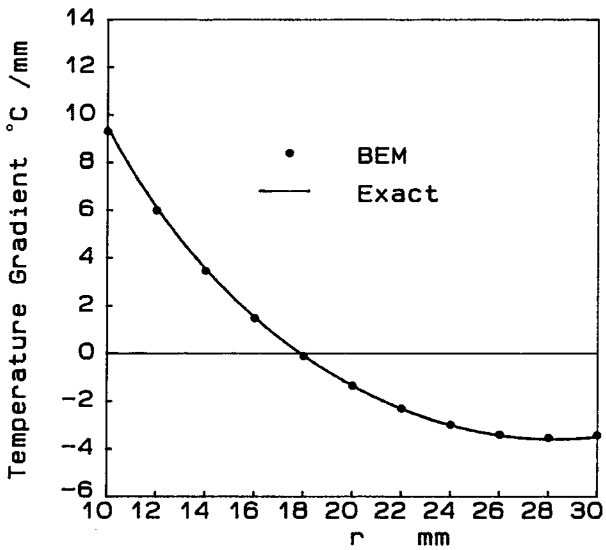

Figure 10 : Temperature gradient

References

Atluri, S. N. (2004): The Meshless Method (MLPG) for Domain & BIE Discretizations, *Tech. Science Press*, Forsyth, GA., 688 pages.

Atluri S. N.; Han Z. D.; Shen, S. (2003): Meshless Local Petrov-Galerkin (MLPG) Approaches for Solving the Weakly-Singular Traction & Displacement Boundary Integral Equations, *CMES: Computer Modeling in Engineering & Sciences*, Vol. 4, No. 5, pp. 507-518.

Atluri, S. N.; Shen S. (2002): The Meshless Local Petrov-Galerkin (MLPG) Method: A Simple Less-costly Alternative to the Finite Element and Boundary Element Methods, *CMES:Computer Methods in Engineering & Sciences*, Vol. 3, No. 1, pp. 11-52.

Brebbia, C. A.; Telles, J. C. F.; Wrobel, L. C. (1984): Boundary Element Techniques - Theory and Applications in Engineering, *Springer - Verlag,*Cpp.46-70.

Davis, P. J.; Rabinowitz, P. (1984): Methods of Numerical Integration, *Academic Press*, pp.344-417, London.

Dyn, N. (1987): Interpolation of Scattered Data by Radial Functions, in Topics in Multivariate Approximation, Eds. C.K Chui, L.L.Schumaker and F.I.Utreras, pp.47-61, , *Academic Press*, London.

Han Z. D.; Atluri S. N. (2003): Truly Meshless Local Petrov-Galerkin (MLPG) Solutions of Traction & Displacement BIEs, *CMES: Computer Modeling in Engineering & Sciences*, Vol. 4, No. 6, pp. 665-678.

Liu, G. R. (2003): Mesh Free Methods, Moving Beyond the Finite Element Method. *CRC Press*, Boca Raton, pp.1-691.

Nowak, A. J.; Neves, A. C. (1994): The Multiple Reciprocity Boundary Element Method, *Computational Mechanics Publication*, Southampton, Boston.

Ochiai, Y.; Sekiya, T. (1995): Steady Thermal Stress Analysis by Improved Multiple-Reciprocity Boundary Element Method, *Journal of Thermal Stresses*, Vol.18, No.6, pp.603-620.

Ochiai, Y.; Sekiya, T. (1996a): Steady Heat Conduction Analysis by Improved Multiple-Reciprocity Boundary Element Method, Engineering Analysis with Boundary Elements, Vol.18, pp.111-117.

Ochiai, Y. (1996b): Generation Method of Distributed Data for FEM Analysis, *JSME International Journal*, Vol.39, No.1 pp.93-98.

Ochiai, Y.; Yasutomi Z. (2000): Improved Method Generating a Free-Form Surface Using Integral Equations, *Computer Aided Geometric Design*, Vol.17, pp.233-245.

Ochiai, Y.; Kobayashi, T. (2001a): Initial Strain Formulation without Internal Cells for Elastoplastic Analysis by Triple-Reciprocity BEM, *International Journal for Numerical Method in Engineering*, 50, 1877-1892.

Ochiai, Y. (2001b): Engineering Analysis with Boundary Elements, *Multidimensional Interpolation and Numerical Integration by Boundary Element Method*, Vol.25, pp.697-704.

Ochiai, Y. (2001c): Steady Heat Conduction Analysis in Orthotropic Bodies by Triple-Reciprocity BEM, *Computer Modeling in Engineering & Sciences*, Vol.2, No.4, pp.435-445,

Ochiai, Y. (2001d): Solid Modeling Using Boundary Integral Equations, *Geometric Modeling*, Ed. F.Kimura, Kluwer, pp.209-220.

Partrige, P. W.; Brebbia, C. A.; Wrobel, L. C. (1991): The Dual Reciprocity Boundary Element Method, *CMP*.

Welch, W.; Witkin, A. (1992): Variational Surface Modeling, *Computer Graphics*, Vol.26, No.2, pp.157-166.